

**ELASTIC INSTABILITY PREDICTIONS FOR DOUBLY-CURVED SHELLS**

Richard H. Gallagher\* and Henry T. Y. Yang\*\*  
Cornell University

Stiffness equations are formulated in representation of the elastic instability behavior of a doubly-curved thin shell element. The element is in the form of a shell of translation of constant thickness and constant principal radii of curvature. The derived relationships are expressed in curvilinear coordinates. An approximate method of eliminating unwanted degrees of freedom from the statement of the buckling eigenvalue problem is applied. Illustrative examples cover the utilization of the element in plate, cylinder, and doubly curved shell elastic instability problems with known solutions. Related comparisons assess the accuracy of the basic formulation, the approximate reduction procedure, and the ability of the present formulation to deal with special features of cylinder buckling.

---

\*Professor of Civil Engineering

\*\*Graduate Student, Department of Structural Engineering

SECTION I  
INTRODUCTION

Problems of elastic instability analysis for thin shell structures have long been of primary concern to aerospace designers and it is not uncommon for considerations related to this model of failure to govern the design of over one-half of the airframe structural weight. Despite these factors, many problems remain in the accurate prediction of the buckling mode of failure of numerous practical components. Reliable analysis tools are unavailable for a circumstance as common as the flat plate with a large reinforced cutout. Other problems, particularly the cylinder in axial compression, involve simple forms of geometry and load but due to the highly nonlinear character of the actual buckling mechanism and its relationship to fabrication inaccuracies, a reasonable correspondence between theory and test is lacking.

A means for the resolution of the above-cited difficulties resides in the finite element method. Development of the method has been motivated, in part, by its ability to model accurately the most complex geometries, load conditions, and behavior mechanisms. The objective of this paper, therefore, is an extension of such capabilities to problems of thin shell instability, using for this purpose a doubly curved shell element. The explicit relationships to be derived are in the class of "linear stability" formulations.

It is pertinent to examine briefly the range of applicability of linear stability analysis in the related areas of practical design. Flat plate buckling can be treated realistically by examination of the bifurcation of the equilibrium state. Here, as noted above, there is a need for capabilities beyond those furnished by traditional methods.

The difficulties attendant upon accurate buckling predictions for curved shell structures stem from a number of sources, each necessitating the inclusion of certain nonlinear terms in analysis and, in all, requiring substantial modification and extension of the total computational process. Understanding of these facets in finite element analysis continues to emerge, as evidenced by recent literature (References 1, and 2). These factors, plus the random nature of the data describing fabrication inaccuracy, has forestalled precise and economically feasible analysis of many shell stability problems.

The importance, therefore, of the linear solution as a basis against which experimentally-determined coefficients are applied is not yet significantly diminished and can be expected to remain so in the near future. In this connection, a means for determining the influence on the linear stability solution of cutouts, stiffening, irregularly distributed loads, and numerous other aspects of practical design is of considerable value. Also, situations exist (e. g., the pressurized shell) for which the linear solution represents actual behavior.

Past developments related to the objective of a formulation of linear stability relationships for the doubly curved shell element have progressed along largely independent paths. On one hand, work in elastic instability analysis within the general framework of the finite element method had advanced rapidly in recent years. Efforts prior to the first AFIT Conference on Matrix Methods in Structural Mechanics were aptly summarized by H. C. Martin (Reference 3) in the Conference proceedings. Since then, papers which have appeared included an explicit formulation of the stability matrices for a rectangular plate in flexure (Reference 4) a general development of finite element procedures for linear shell stability analysis with use of flat triangular and quadrilateral plate elements (Reference 5) and an extension of the doubly curved axisymmetric shell element to represent stability problems of that restricted class of geometric and load condition. (Reference 6)

Interest has likewise been strong in the formulation of basic (i. e., excluding elastic instability) stiffnesses for curved thin shell finite elements. This interest has been prompted, in large measure, by questions raised in References 7 and 8 and elsewhere as to the adequacy of flat plate or straight line elements in representation of the behavior of curved structures. In one group of articles (References 9, 10, and 11) attention was given to the cylindrical shell element. It should be noted that Reference 9 emphasizes geometric nonlinearity and includes the terms for linear stability as a special case. Doubly curved elements are formulated in References 12 through 16. A useful summary of progress to date in the special area of the axisymmetric shell element is presented in Reference 7.

The present development constitutes an extension of the formulation (Reference 12) for the doubly curved shell element shown in Figure 1. Concepts developed in References 5 and 18 for the formulation of finite element stiffness equations to represent elastic instability effects are applied herein. The component aspects of the formulative procedure consist of the establishment of pertinent potential energy expressions, definition of the element geometry and assumed displacement fields, and derivation of the desired relationships in algebraic form. Considerations underlying each of these steps are examined in the following sections.

## SECTION II

### ELEMENT GEOMETRY

A description of the element geometry (Figure 1) describes a differential element of the structure as well. The element is of constant thickness ( $t$ ) and possesses constant radii of curvature ( $R_1, R_2$ ) corresponding to the curvilinear coordinates of the middle surface,  $\alpha_1$  and  $\alpha_2$ , respectively. The sides of the element lie along or parallel to the curvilinear coordinate direction and are of length  $a$  and  $b$ , as shown. The element corner points are numbered from 1 to 4 in counterclockwise order.

Lamé parameters ( $A_1, A_2$ ) serve to relate the curvilinear and system ( $x, y, z$ ) coordinates. Thus,

$$\begin{aligned} A_1^2 &= \left(\frac{\partial x}{\partial \alpha_1}\right)^2 + \left(\frac{\partial y}{\partial \alpha_1}\right)^2 + \left(\frac{\partial z}{\partial \alpha_1}\right)^2 \\ A_2^2 &= \left(\frac{\partial x}{\partial \alpha_2}\right)^2 + \left(\frac{\partial y}{\partial \alpha_2}\right)^2 + \left(\frac{\partial z}{\partial \alpha_2}\right)^2 \end{aligned} \quad (1)$$

and the respective special forms of the element yield:

$$\begin{array}{lll} \text{Doubly - curved} & A_1 = R_1 & A_2 = R_2 \\ \text{Singly - curved} & A_1 = 1 & A_2 = R \\ \text{Flat Plate} & A_1 = 1 & A_2 = 1 \end{array} \quad (2)$$

In utilizing the internal force distribution, it is convenient to utilize line loading statically equivalent to the internal stresses, as in Figure 2.

Six generalized forces act at each of the element corners. Five of these are the conventional direct forces (3 in number) and bending moments (2 in number). The sixth generalized force, whose counterpart generalized displacement corresponds to the twist derivative  $\left(\frac{\partial^2 w}{\partial \alpha_1 \partial \alpha_2}\right)$  will be described in conjunction with the discussion of the assumed displacement field.

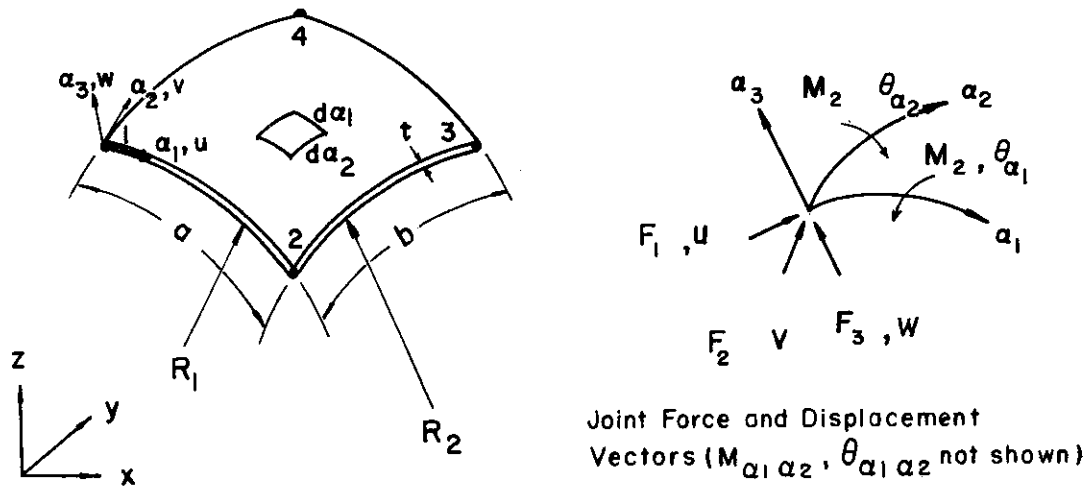
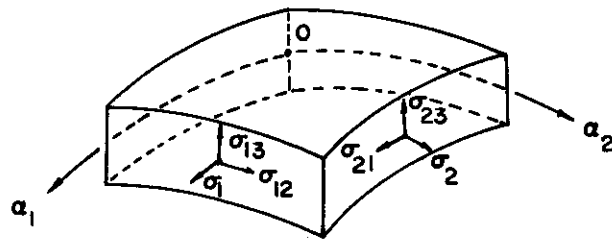
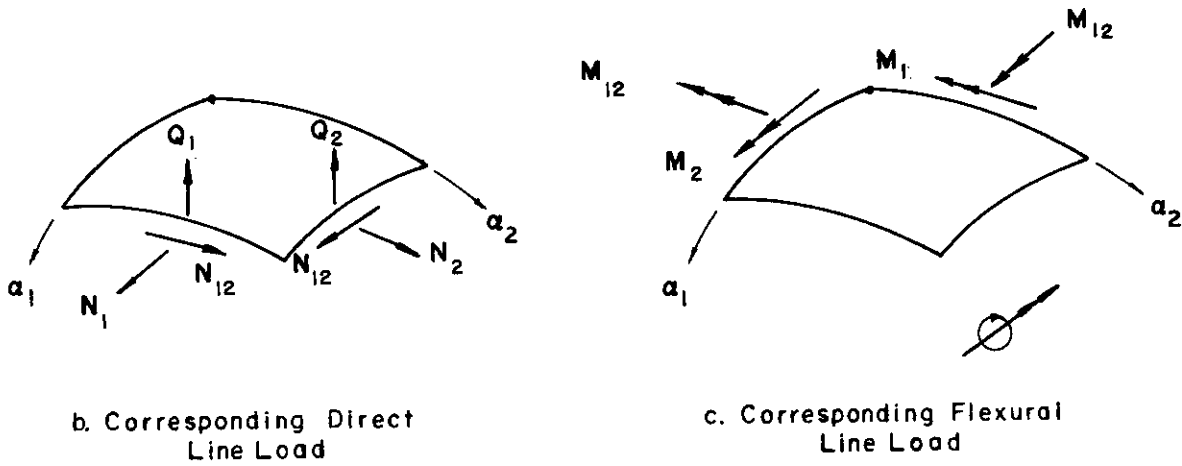


Figure 1. Element Geometry



a. Stress Components



b. Corresponding Direct Line Load

c. Corresponding Flexural Line Load

Figure 2. Internal Stress Components

SECTION III  
FORMULATION OF POTENTIAL ENERGY FUNCTION

The subject development of element stiffness relationships is based upon application of the Minimum Potential Energy Theorem. It is therefore necessary to construct an expression for the potential energy function in terms of the shell displacements and displacement derivatives. Assumptions underlying this derivation are as follows:

- (1) The material is elastic and transversely isotropic.
- (2) The shell middle surface bisects the thickness.
- (3) Strains vary linearly in the thickness direction.
- (4) Transverse shear strains and direct stresses in the  $\alpha_3$  direction are neglected.
- (5) The normal displacement ( $w$ ) is a function only of the middle surface coordinates, i.e.,  $w = w(\alpha_1, \alpha_2)$ .

The derived strain-displacement relationships are an extension of those due to Novozhilov, (Reference 17) in this case the quadratic terms in their displacements and their derivatives being retained. Terms higher than second order are discarded. Reference 19 formulates the strain-displacement relationships shown in Figure 3.

The expression for potential energy ( $\Pi_p$ ) is

$$\Pi_p = U - W \tag{3}$$

where

$$U = \frac{1}{2} \int_V (\sigma_1 \epsilon_1 + \sigma_2 \epsilon_2 + \sigma_{12} \omega) dV \tag{4}$$

$$W = - \int_V (\bar{\sigma}_1 \epsilon + \bar{\sigma}_2 \epsilon + \bar{\sigma}_{12} \omega) dV \tag{5}$$

In forming an expression appropriate to the elastic instability condition, the distinction is made that the stresses  $\sigma_1, \sigma_2$  and  $\sigma_{12}$  in  $U$  vary linearly through the deformation, while the stresses in  $W$ , the values  $\bar{\sigma}_1, \bar{\sigma}_2$  and  $\bar{\sigma}_{12}$ , are constant initial stresses and are equal to their values at the final equilibrium state. If the equilibrium state is neutral equilibrium, the stresses  $\bar{\sigma}_1, \bar{\sigma}_2$  and  $\bar{\sigma}_{12}$  are the buckling stresses.

The derivation of the strain energy portion (U) of the potential energy, based on the linear portions of the strain-displacement equations (Figure 3), is detailed in Reference 12. Attention is turned here to the formulation of the (W) portion of the potential energy, which is subsequently operated upon to yield the "incremental" element stiffness matrix representative of elastic instability effects. As shown in Reference 19, the basic form of this portion of the potential energy can be written

$$\begin{aligned}
 W = & N_1 \int_A \epsilon_{\alpha 1} ds_1 ds_2 + M_1 \int_A K_1 ds_1 ds_2 \\
 & + N_2 \int_A \epsilon_{\alpha 2} ds_1 ds_2 + M_2 \int_A K_2 ds_1 ds_2 \\
 & + N_{12} \int_A \omega ds_1 ds_2 + M_{12} \int_A K_{12} ds_1 ds_2
 \end{aligned} \tag{6}$$

By substitution into this equation of the strain-displacement equations of Figure 3, and with the disregard of first-order terms in the displacements and their derivatives, one obtains

$$W = W_{mm} + W_{fm} + W_{ff} \tag{7}$$

where the individual terms  $W_{mm}$ ,  $W_{ff}$  and  $W_{fm}$  are presented in detail in Figure 4. This segregation of the terms in the complete function W is made with reference to membrane displacements and their derivatives ( $W_{mm}$ ), the flexural displacements and their derivatives ( $W_{ff}$ ), and cross products of these ( $W_{mf}$ ). These expressions can be employed in derivation of the desired stiffness equations once the element displacement fields have been assumed.

### Middle Surface Strains

$$\begin{aligned}\epsilon_{\alpha_1} &= \frac{\partial u}{\partial s_1} + \frac{w}{R_1} + \frac{1}{2} \left( \frac{\partial v}{\partial s_1} \right)^2 + \frac{1}{2} \left( \frac{u}{R_1} - \frac{\partial w}{\partial s_1} \right)^2 \\ \epsilon_{\alpha_2} &= \frac{\partial v}{\partial s_2} + \frac{w}{R_2} + \frac{1}{2} \left( \frac{\partial u}{\partial s_2} \right)^2 + \frac{1}{2} \left( \frac{v}{R_2} - \frac{\partial w}{\partial s_2} \right)^2 \\ \omega &= \frac{\partial u}{\partial s_2} + \frac{\partial v}{\partial s_1} - \left( \frac{\partial u}{\partial s_1} \right) \left( \frac{\partial v}{\partial s_1} \right) - \left( \frac{\partial v}{\partial s_1} \right) \left( \frac{w}{R_1} \right) + \left( \frac{\partial w}{\partial s_1} \right) \left( \frac{\partial w}{\partial s_2} \right) - \left( \frac{v}{R_2} \right) \left( \frac{\partial w}{\partial s_1} \right) \\ &\quad - \left( \frac{u}{R_1} \right) \left( \frac{\partial w}{\partial s_2} \right) + \left( \frac{u}{R_1} \right) \left( \frac{v}{R_2} \right) - \left( \frac{\partial u}{\partial s_2} \right) \left( \frac{\partial v}{\partial s_2} \right) - \left( \frac{\partial u}{\partial s_2} \right) \left( \frac{w}{R_2} \right)\end{aligned}$$

Strains of a Surface at a Distance  $z$  from and Parallel to the Middle Surface

$$\begin{aligned}\epsilon_{\alpha_1}^{(z)} &= \epsilon_{\alpha_1} + \kappa_1 z + \lambda_1 z^2 \\ \epsilon_{\alpha_2}^{(z)} &= \epsilon_{\alpha_2} + \kappa_2 z + \lambda_2 z^2 \\ \omega^{(z)} &= \omega + \kappa_{12} z + \lambda_{12} z^2\end{aligned}$$

Where

$$\begin{aligned}\kappa_1 &= \frac{\partial^2 w}{\partial s_1^2} \left( -1 + \frac{\partial u}{\partial s_1} + \frac{w}{R_1} \right) - \frac{1}{R_1} \left\{ \frac{w}{R_1} + \frac{1}{2} \left\{ \left( \frac{\partial u}{\partial s_2} + \frac{\partial v}{\partial s_1} \right)^2 + \left( \frac{u}{R_1} - \frac{\partial w}{\partial s_1} \right)^2 - \left( \frac{v}{R_2} - \frac{\partial w}{\partial s_2} \right)^2 \right\} - \left( \frac{\partial w}{\partial s_1} \right)^2 \right. \\ &\quad \left. + \left( \frac{\partial u}{\partial s_1} \right)^2 + \left( \frac{\partial v}{\partial s_1} \right)^2 + \left( \frac{\partial u}{\partial s_1} \right) \left( \frac{w}{R_1} \right) + \left( \frac{\partial w}{\partial s_1} \right) \left( \frac{u}{R_1} \right) \right\} \\ \kappa_2 &= \frac{\partial^2 w}{\partial s_2^2} \left( -1 + \frac{\partial v}{\partial s_2} + \frac{w}{R_2} \right) - \frac{1}{R_2} \left\{ \frac{w}{R_2} - \frac{1}{2} \left\{ \left( \frac{\partial u}{\partial s_2} + \frac{\partial v}{\partial s_1} \right)^2 + \left( \frac{u}{R_1} - \frac{\partial w}{\partial s_1} \right)^2 + \left( \frac{v}{R_2} - \frac{\partial w}{\partial s_2} \right)^2 \right\} - \left( \frac{\partial w}{\partial s_2} \right)^2 \right. \\ &\quad \left. + \left( \frac{\partial v}{\partial s_2} \right)^2 + \left( \frac{\partial u}{\partial s_2} \right)^2 + \left( \frac{\partial v}{\partial s_2} \right) \left( \frac{w}{R_2} \right) + \left( \frac{\partial w}{\partial s_2} \right) \left( \frac{v}{R_2} \right) \right\} \\ \lambda_1 &= \frac{1}{2} \left\{ \frac{\partial^2 w}{\partial s_1 \partial s_2} + \left( \frac{1}{R_1} - \frac{1}{R_2} \right) \left( \frac{\partial v}{\partial s_1} \right) \right\}^2 \\ \lambda_2 &= \frac{1}{2} \left\{ \frac{\partial^2 w}{\partial s_1 \partial s_2} + \left( \frac{1}{R_2} - \frac{1}{R_1} \right) \left( \frac{\partial u}{\partial s_2} \right) \right\}^2 \\ \kappa_{12} &= 2 \left\{ \frac{\partial^2 w}{\partial s_1 \partial s_2} \left( -1 + \frac{\partial u}{\partial s_1} + \frac{\partial v}{\partial s_2} + \frac{w}{R_1} + \frac{w}{R_2} \right) + \frac{\partial^2 u}{\partial s_1 \partial s_2} \left( \frac{\partial w}{\partial s_1} - \frac{u}{R_1} \right) + \frac{\partial^2 v}{\partial s_1 \partial s_2} \left( \frac{\partial w}{\partial s_2} - \frac{v}{R_2} \right) + \frac{1}{2} \left( \frac{\partial u}{\partial s_2} + \frac{\partial v}{\partial s_1} \right) \left( \frac{\partial^2 w}{\partial s_1^2} + \frac{\partial^2 w}{\partial s_2^2} \right) \right. \\ &\quad \left. - \frac{1}{R_1} \left\{ \frac{\partial v}{\partial s_1} - \frac{\partial u}{\partial s_2} - \left( \frac{\partial u}{\partial s_1} \right) \left( \frac{\partial w}{\partial s_2} \right) + 2 \left( \frac{\partial u}{\partial s_1} \right) \left( \frac{\partial v}{\partial s_2} \right) - \left( \frac{\partial u}{\partial s_1} \right) \left( \frac{\partial v}{\partial s_1} \right) + \left( \frac{\partial u}{\partial s_1} \right) \left( \frac{\partial w}{\partial s_1} \right) + \left( \frac{\partial v}{\partial s_2} \right) \left( \frac{w}{R_2} \right) + \left( \frac{u}{R_1} \right) \left( \frac{\partial w}{\partial s_2} \right) - 2 \left( \frac{\partial v}{\partial s_1} \right) \left( \frac{w}{R_1} \right) \right\} \\ &\quad \left. - \frac{1}{R_2} \left\{ \frac{\partial u}{\partial s_2} - \frac{\partial v}{\partial s_1} - \left( \frac{\partial v}{\partial s_2} \right) \left( \frac{\partial w}{\partial s_1} \right) + 2 \left( \frac{\partial v}{\partial s_2} \right) \left( \frac{\partial u}{\partial s_1} \right) - \left( \frac{\partial v}{\partial s_2} \right) \left( \frac{\partial u}{\partial s_2} \right) + \left( \frac{\partial v}{\partial s_2} \right) \left( \frac{\partial w}{\partial s_2} \right) + \left( \frac{\partial v}{\partial s_2} \right) \left( \frac{w}{R_2} \right) + \left( \frac{\partial v}{\partial s_2} \right) \left( \frac{u}{R_1} \right) + \left( \frac{v}{R_2} \right) \left( \frac{\partial w}{\partial s_1} \right) - 2 \left( \frac{\partial u}{\partial s_2} \right) \left( \frac{w}{R_2} \right) \right\} \right\} \\ \lambda_{12} &= \left\{ \left( \frac{1}{R_2} - \frac{1}{R_1} \right) \frac{\partial v}{\partial s_1} - \frac{\partial^2 w}{\partial s_1 \partial s_2} \right\} \left( \frac{\partial^2 w}{\partial s_1^2} + \frac{w}{R_1^2} \right) + \left\{ \left( \frac{1}{R_1} - \frac{1}{R_2} \right) \frac{\partial u}{\partial s_2} - \frac{\partial^2 w}{\partial s_1 \partial s_2} \right\} \left( \frac{\partial^2 w}{\partial s_2^2} - \frac{w}{R_2^2} \right)\end{aligned}$$

Note:  $s_1 = A_1 \alpha_1$ ,  $s_2 = A_2 \alpha_2$

Figure 3. Strain-Displacement Equations



SECTION IV  
DISPLACEMENT FUNCTIONS

Zienkiewicz and Cheung (Reference 20) summarize conditions to be met by displacement functions chosen in representation of element behavior for the purpose of matrix displacement analyses. These conditions require: (1) Inclusion of rigid-body-motion and constant strain states in the chosen functions, and (2) Satisfaction of interelement continuity of displacement across element boundaries in the complete analytical model. One can demand more stringent conditions, for example, retention of geometric symmetry in the chosen function, or representation of all terms of a given order of polynomial in the functions.

Since the element under study is a generalization, in curvilinear coordinates, of the flat rectangular plate element, it is convenient to seek a basis for the selection of displacement fields from the latter. The advantages gained from drawing from past efforts may include the direct statement of the functions in terms of the element joint degrees of freedom, rather than in terms of undetermined parameters, and insight gained from previous investigations of the consequences of violating certain of the above conditions, where such violations enable the use of functions which permit more convenient formulations. Both of these circumstances exist here.

The chosen functions are as follows:

$$u = \frac{1}{ab} \left[ (\alpha_1 - a)(\alpha_2 - b) u_1 - \alpha_1(\alpha_2 - b) u_2 + \alpha_1 \alpha_2 u_3 - (\alpha_1 - a) \alpha_2 u_4 \right] \quad (8)$$

$$v = \frac{1}{ab} \left[ (\alpha_1 - a)(\alpha_2 - b) v_1 - \alpha_1(\alpha_2 - b) v_2 + \alpha_1 \alpha_2 v_3 - (\alpha_1 - a) \alpha_2 v_4 \right] \quad (9)$$

$$\begin{aligned} w = & \left[ (a^3 + 2\alpha_1^3 - 3a\alpha_1^2)(b^3 + 2\alpha_2^3 - 3b\alpha_2^2) w + (3a\alpha_1^2 - 2\alpha_1^3)(b^3 + 2\alpha_2^3 - 3b\alpha_2^2) w_2 \right. \\ & + (3a\alpha_1^2 - 2\alpha_1^3)(3b\alpha_2^2 - 2\alpha_2^3) w_3 + (a^3 + 2\alpha_1^3 - 3a\alpha_1^2)(3b\alpha_2^2 - 2\alpha_2^3) w_4 \\ & + a\alpha_1(a_1 - a)^2(b^3 + 2\alpha_2^3 - 3b\alpha_2^2) \theta\alpha_1 + a(\alpha_1^3 - a\alpha_1^2)(b^3 + 2\alpha_2^3 - 3b\alpha_2^2) \theta\alpha_{1,2} \\ & + a(\alpha_1^3 - a\alpha_1^2)(3b\alpha_2^2 - 2\alpha_2^3) \theta\alpha_{1,3} + a(\alpha_1 - a)^2 \alpha_1(3b\alpha_2^2 - 2\alpha_2^3) \theta\alpha_{1,4} \\ & + b(a^3 + 2\alpha_1^3 - 3a\alpha_1^2) \alpha_2(\alpha_2 - b)^2 \theta\alpha_{2,1} + b(3a\alpha_1^2 - 2\alpha_1^3) \alpha_2(\alpha_2 - b)^2 \theta\alpha_{2,2} \\ & + b(3a\alpha_1^2 - 2\alpha_1^3)(\alpha_2^3 - b\alpha_2^2) \theta\alpha_{2,3} + b(a^3 + 2\alpha_1^3 - 3a\alpha_1^2)(\alpha_2^3 - b\alpha_2^2) \theta\alpha_{2,4} \\ & + ab\alpha_1 \alpha_2 (\alpha_1 - a)^2 (\alpha_2 - b)^2 \theta\alpha\alpha_1 + ab\alpha_1 \alpha_2 (\alpha_1 - a) (\alpha_2 - b)^2 \theta\alpha\alpha_2 \\ & \left. + ab\alpha_1 \alpha_2 (\alpha_1^2 - a\alpha_1)(\alpha_2^2 - b\alpha_2) \theta\alpha\alpha_3 + ab\alpha_1 \alpha_2 (\alpha_1 - a)^2 (\alpha_2^2 - b\alpha_2) \theta\alpha\alpha_4 \right] \div a^3 b^3 \quad (10) \end{aligned}$$

These functions possess geometric symmetry and meet conditions (1) and (2) cited above, for the rectangular flat plate, but do not include all terms in the maximum order of polynomial represented therein. The function for flexural behavior is of particular interest since it introduces a "special" degree of freedom at each joint, the parameter  $\theta_{\alpha_1 \alpha_2}$  which is the twist derivative  $\frac{\partial^2 w}{\partial \alpha_1 \partial \alpha_2}$ . The multipliers of the other joint displacements ( $w, \theta_{\alpha_1}, \theta_{\alpha_2}$ ) can be recognized as either the function generated in consequence of a Hermitian polynomial procedure, (Reference 21) or as the "crossing" of the functions related to beam flexural behavior in the  $\alpha_1$  and  $\alpha_2$  directions, respectively. Taking the latter view, one finds that simple twisting action is absent from among the multipliers of the first 12 terms of Equation 10, i.e., the term  $\alpha_1 \alpha_2$  nowhere appears in these. Inclusion of the twist degree of freedom enables presentation of the needed term.

Satisfaction of conditions related to rigid body motion and the continuity of displacement across element boundaries in the assembled idealization are immediately violated by the present element in the curvilinear structure. The net displacements along a juncture line are in general a combination of the  $u$ ,  $v$ , and  $w$  displacements. The  $u$  and  $v$  displacements are of linear form while the  $w$  displacements are of cubic variation. Similar considerations influence the satisfaction of the rigid body motion requirement.

Lack of satisfaction of the interelement continuity of displacement requirement has not been identified, per se, as a source of convergence difficulties in this class of problem although, with violation of this and the other cited condition, guarantees relative to monotonicity of convergence and of a lower-bound strain energy solution are lost.

Attention has been given to the representation of rigid body displacement in curved shell finite element analysis by both Haisler and Stricklin (Reference 22) and by Clough and Cantin (Reference 9). Reference 22 examines the violation of the subject condition with reference to axisymmetric thin shell element and, through numerical evaluation, conclude that convergence to the classical solution of the problems tested is not prevented, nor is the accuracy of the solution prejudiced significantly for refined idealizations. Reference 9, in the formulation of a cylindrical shell element, conducts a similar study. Although the view that convergence in the limit is not compromised is reinforced, the discrepancies due to exclusion of rigid body modes appear to be more significant at any given level of computational effort. Clearly, the extent to which an element sustains rigid body motion in a specific problem will govern the significance of this factor.

In order to satisfy the conditions related to rigid body motion, Clough and Cantin adopt a displacement function in terms of undetermined parameters and the appropriate trigonometric functions of the subtended angle of the cylinder segment. Adaptation of this to the subject element would introduce considerably greater complexity into the formulative effort. The numerical comparisons of Section VII constitute, in part, an assessment of the adopted simpler approach.

SECTION V  
FORMULATION OF ELEMENT AND COMPLETE SYSTEM

The assumptions of the previous section relative to element displacement behavior can be symbolized as follows:

$$u = f_1 u_1 + f_2 u_2 + f_3 u_3 + f_4 u_4 = f u \quad (11)$$

$$v = f_1 v_1 + f_2 v_2 + f_3 v_3 + f_4 v_4 = f v \quad (12)$$

$$w = f_9 w_{10} f_2 w_2 + \dots + f_{24} \theta_{\alpha_1 \alpha_2} = f w \begin{bmatrix} w \\ \theta_{\alpha_1} \\ \theta_{\alpha_2} \\ \theta_{\alpha_1 \alpha_2} \end{bmatrix} \quad (13)$$

and, by introduction of these into Equation 3 and performance of the detailed differentiations and integrations as are indicated in Figure 4 and elsewhere in the preceding section, one obtains an expression for the element potential energy of the form

$$\begin{aligned} &\text{with, } \{ u_e, v_e, w_e, \theta_{\alpha_{1e}}, \theta_{\alpha_{2e}}, \theta_{\alpha_1 \alpha_{2e}} \} = \Delta_e \\ &\quad \{ F_{\alpha_{1e}}, F_{\alpha_{2e}}, F_{\alpha_{3e}}, M_{\alpha_{1e}}, M_{\alpha_{2e}}, M_{\alpha_1 \alpha_{3e}} \} = F_e \\ \Pi_{P_e} &= \frac{\Delta_e^T}{2} k_e \Delta_e + \frac{\Delta_e^T}{2} n_e \Delta_e - \Delta_e^T F_e \end{aligned} \quad (14)$$

where the subscript 'e' designates the respective matrices as measures of the behavior of a single element.

$$W = W_{mm} + W_{mf} + W_{ff}$$

where

$$\begin{aligned} W_{mm} = & \frac{1}{2} N_1 \int_A \left\{ \left( \frac{\partial V}{\partial \delta_1} \right)^2 + \left( \frac{U}{R_1} \right)^2 \right\} d\delta_1 d\delta_2 + \frac{1}{2} N_2 \int_A \left\{ \left( \frac{\partial U}{\partial \delta_2} \right)^2 + \left( \frac{V}{R_2} \right)^2 \right\} d\delta_1 d\delta_2 \\ & - \frac{1}{2} \left( \frac{M_1}{R_1} + \frac{M_2}{R_2} \right) \int_A \left\{ \left( \frac{\partial U}{\partial \delta_2} \right)^2 + \left( \frac{\partial V}{\partial \delta_1} \right)^2 + 2 \left( \frac{\partial U}{\partial \delta_2} \right) \left( \frac{\partial V}{\partial \delta_1} \right) + \left( \frac{U}{R_1} \right)^2 + \left( \frac{V}{R_2} \right)^2 \right\} d\delta_1 d\delta_2 \\ & - \frac{M_1}{R_1} \int_A \left\{ \left( \frac{\partial U}{\partial \delta_1} \right)^2 + \left( \frac{\partial V}{\partial \delta_1} \right)^2 \right\} d\delta_1 d\delta_2 - \frac{M_2}{R_2} \int_A \left\{ \left( \frac{\partial U}{\partial \delta_2} \right)^2 + \left( \frac{\partial V}{\partial \delta_2} \right)^2 \right\} d\delta_1 d\delta_2 \\ & - N_{12} \int_A \left\{ \left( \frac{\partial U}{\partial \delta_1} \right) \left( \frac{\partial V}{\partial \delta_1} \right) - \left( \frac{U}{R_1} \right) \left( \frac{V}{R_2} \right) + \left( \frac{\partial U}{\partial \delta_2} \right) \left( \frac{\partial V}{\partial \delta_2} \right) \right\} d\delta_1 d\delta_2 \\ & - M_{12} \int_A \left\{ 2 \left( \frac{\partial U}{\partial \delta_1 \partial \delta_2} \right) \left( \frac{U}{R_1} \right) + 2 \left( \frac{\partial^2 V}{\partial \delta_1 \partial \delta_2} \right) \left( \frac{V}{R_2} \right) + \frac{2}{R_1} \left( \frac{\partial U}{\partial \delta_1} \right) \left( \frac{\partial U}{\partial \delta_2} \right) + \frac{2}{R_2} \left( \frac{\partial V}{\partial \delta_1} \right) \left( \frac{\partial V}{\partial \delta_2} \right) \right. \\ & \quad \left. - \left( \frac{1}{R_1} - \frac{1}{R_2} \right) \left[ \left( \frac{\partial U}{\partial \delta_1} \right) \left( \frac{\partial V}{\partial \delta_1} \right) - \left( \frac{\partial U}{\partial \delta_2} \right) \left( \frac{\partial V}{\partial \delta_2} \right) \right] \right\} d\delta_1 d\delta_2 \end{aligned}$$

$$\begin{aligned} W_{mf} = & -N_1 \int_A \left( \frac{U}{R_1} \right) \left( \frac{\partial W}{\partial \delta_1} \right) d\delta_1 d\delta_2 - N_2 \int_A \left( \frac{V}{R_2} \right) \left( \frac{\partial W}{\partial \delta_2} \right) d\delta_1 d\delta_2 \\ & + M_1 \int_A \left\{ \left( \frac{\partial^2 W}{\partial \delta_1^2} \right) \left( \frac{\partial U}{\partial \delta_1} \right) + \frac{1}{R_1} \left( \frac{V}{R_2} \right) \left( \frac{\partial W}{\partial \delta_2} \right) - \left( \frac{\partial U}{\partial \delta_1} \right) \left( \frac{W}{R_1} \right) \right\} d\delta_1 d\delta_2 \\ & + M_2 \int_A \left\{ \left( \frac{\partial^2 W}{\partial \delta_2^2} \right) \left( \frac{\partial V}{\partial \delta_2} \right) + \frac{1}{R_2} \left( \frac{U}{R_1} \right) \left( \frac{\partial W}{\partial \delta_1} \right) - \left( \frac{\partial V}{\partial \delta_2} \right) \left( \frac{W}{R_2} \right) \right\} d\delta_1 d\delta_2 \\ & - N_{12} \int_A \left\{ \left( \frac{\partial U}{\partial \delta_2} \right) \left( \frac{W}{R_2} \right) + \left( \frac{\partial V}{\partial \delta_1} \right) \left( \frac{W}{R_1} \right) + \left( \frac{\partial W}{\partial \delta_1} \right) \left( \frac{V}{R_2} \right) + \left( \frac{\partial W}{\partial \delta_2} \right) \left( \frac{U}{R_1} \right) \right\} d\delta_1 d\delta_2 \\ & + M_{12} \int_A \left\{ 2 \left( \frac{\partial^2 W}{\partial \delta_1 \partial \delta_2} \right) \left( \frac{\partial U}{\partial \delta_1} + \frac{\partial V}{\partial \delta_2} \right) + 2 \left( \frac{\partial^2 U}{\partial \delta_1 \partial \delta_2} \right) \left( \frac{\partial W}{\partial \delta_1} \right) + 2 \left( \frac{\partial^2 V}{\partial \delta_1 \partial \delta_2} \right) \left( \frac{\partial W}{\partial \delta_2} \right) \right. \\ & \quad + \left( \frac{\partial U}{\partial \delta_2} + \frac{\partial V}{\partial \delta_1} \right) \left( \frac{\partial^2 W}{\partial \delta_1^2} + \frac{\partial^2 W}{\partial \delta_2^2} \right) + \frac{1}{R_1} \left[ 2 \left( \frac{\partial V}{\partial \delta_1} \right) \left( \frac{W}{R_1} \right) - \left( \frac{\partial U}{\partial \delta_2} \right) \left( \frac{W}{R_1} \right) \right. \\ & \quad \left. - \left( \frac{\partial U}{\partial \delta_2} \right) \left( \frac{W}{R_2} \right) - \left( \frac{U}{R_1} \right) \left( \frac{\partial W}{\partial \delta_2} \right) \right] + \frac{1}{R_2} \left[ 2 \left( \frac{\partial U}{\partial \delta_2} \right) \left( \frac{W}{R_2} \right) - \left( \frac{\partial V}{\partial \delta_1} \right) \left( \frac{W}{R_2} \right) \right. \\ & \quad \left. - \left( \frac{\partial V}{\partial \delta_1} \right) \left( \frac{W}{R_1} \right) - \left( \frac{V}{R_2} \right) \left( \frac{\partial W}{\partial \delta_1} \right) \right] \right\} d\delta_1 d\delta_2 \end{aligned}$$

$$\begin{aligned} W_{ff} = & \frac{1}{2} N_1 \int_A \left( \frac{\partial W}{\partial \delta_1} \right)^2 d\delta_1 d\delta_2 + \frac{1}{2} N_2 \int_A \left( \frac{\partial W}{\partial \delta_2} \right)^2 d\delta_1 d\delta_2 \\ & + \frac{M_1}{R_1} \int_A \left\{ \left( \frac{\partial^2 W}{\partial \delta_1^2} \right) (W) + \frac{1}{2} \left[ \left( \frac{\partial W}{\partial \delta_1} \right)^2 - \left( \frac{\partial W}{\partial \delta_2} \right)^2 \right] \right\} d\delta_1 d\delta_2 \\ & + \frac{M_2}{R_2} \int_A \left\{ \left( \frac{\partial^2 W}{\partial \delta_2^2} \right) (W) + \frac{1}{2} \left[ \left( \frac{\partial W}{\partial \delta_2} \right)^2 - \left( \frac{\partial W}{\partial \delta_1} \right)^2 \right] \right\} d\delta_1 d\delta_2 \\ & + N_{12} \int_A \left( \frac{\partial W}{\partial \delta_1} \right) \left( \frac{\partial W}{\partial \delta_2} \right) d\delta_1 d\delta_2 \\ & + M_{12} \left( \frac{1}{R_1} + \frac{1}{R_2} \right) \int_A \left\{ 2 \left( \frac{\partial^2 W}{\partial \delta_1 \partial \delta_2} \right) (W) + \left( \frac{\partial W}{\partial \delta_1} \right) \left( \frac{\partial W}{\partial \delta_2} \right) \right\} d\delta_1 d\delta_2 \end{aligned}$$

Figure 4. Potential Energy Component Related to Instability Behavior

A detailed statement of the complete sets of stiffness coefficients for these matrices is well beyond the scope of feasible presentation within this paper; explicit formulations for these coefficients are to be found in References 12 and 19. To give an indication of their form, the following coefficients are cited:

The coefficient in  $k_e$  relating  $F_{\alpha_1}$ , and  $u_1$ :

$$k_{1,1} = \frac{b}{3a} \left( D_m + \frac{D_b}{R_1^2} + \frac{a}{6b} \left( D_m + \frac{4D_b}{R_1^2} \right) \right) \quad (15)$$

where  $D_b = \frac{E_b t^3}{12(1-\mu^2)}$  and  $D_m = \frac{(E t)_m}{(1-\mu^2)}$  are the flexural and membrane rigidity respectively, the rest of the symbols are explained in Figures 1 and 2.

The coefficient in  $k_e$  relating  $F_{\alpha_1}$  and  $w_1$ :

$$k_{1,9} = \frac{7b}{40} D_m \left( \frac{1}{R_1} + \frac{\mu}{R_2} \right) - \frac{\mu D_b}{2bR_1} + \frac{(1-\mu) D_b}{bR_1} \quad (16)$$

The coefficient in  $n_e$  relating  $F_{\alpha_3}$  and  $W_1$ :

$$n_{9,9} = \frac{78}{175} \left[ \left( \frac{b}{a} N_1 + \frac{a}{b} N_2 \right) - \left( \frac{a}{b} + \frac{b}{a} \right) \left( \frac{M_1}{R_1} + \frac{M_2}{R_2} \right) \right] + \frac{N_{12}}{2} - \frac{3}{2} \left( \frac{1}{R_1} + \frac{1}{R_2} \right) M_{12} \quad (17)$$

where  $a$ ,  $b$ ,  $R_1$ ,  $R_2$ ,  $N_1$ ,  $N_2$ ,  $M_1$ , and  $M_2$  are explained in Figures 1 and 2. For infinite values of the radii  $R_1$  and  $R_2$  the Expressions (15) and (16) reduce to well-known stiffness coefficients for the rectangular flat plate.

In order to study aspects of the solution for the behavior of the complete structure, consider the idealization of such a structure to be formed solely of the subject elements. In this case the Equations 14 for the respective elements can be combined in an appropriate manner to form the system potential energy:

$$\Pi_p = \frac{\Delta^T}{2} K \Delta + \frac{\Delta^T}{2} N \Delta - \Delta^T P \quad (18)$$

In accordance with the theorem of minimum potential energy, the first variation of  $\Pi_p$  for a stable system is equal to zero, corresponding to the requirement that for any virtual displacement the change in the total potential energy of the system is positive. Thus,  $\delta \Pi_p = 0$ , and when applied to Equation 18 it yields

$$K \Delta + N \Delta = P \quad (19)$$

The solution to this equilibrium problem cannot be obtained directly in the case of the curved shell, due to the dependence of the coefficients of  $\mathbf{N}$  upon the internal force distribution, which itself depends upon the total solution. Defining the partition of the matrices in Equation 19 as follows:

$$\left[ \begin{array}{c|c} \mathbf{K}_{11} & \mathbf{K}_{12} \\ \hline & \\ \mathbf{K}_{21} & \mathbf{K}_{22} \end{array} \right] \begin{bmatrix} u \\ v \\ w \\ \theta_{\alpha_1} \\ \theta_{\alpha_2} \\ \theta_{\alpha\alpha} \end{bmatrix} + \left[ \begin{array}{c|c} \mathbf{N}_{11} & \mathbf{N}_{12} \\ \hline & \\ \mathbf{N}_{21} & \mathbf{N}_{22} \end{array} \right] = \begin{bmatrix} \mathbf{P}_1 \\ \mathbf{P}_2 \\ \mathbf{P}_3 \\ \mathbf{M}_1 \\ \mathbf{M}_2 \\ \mathbf{M}_{12} \end{bmatrix} \quad (20)$$

it can be noted that for the flat plate case  $\mathbf{N}_{11} = \mathbf{N}_{12} = \mathbf{N}_{21} = \mathbf{0}$  and the matrix  $\mathbf{N}_{22}$  contains terms derivable only from the  $u$  and  $v$  displacements. In this special case, since the latter can now be calculated independently of  $w, \theta_{\alpha_1}, \theta_{\alpha_2}, \theta_{\alpha_1\alpha_2}$ , the solution can be accomplished directly.

Turning now to stability analysis, the required condition is that at the critical load there exist nonzero "perturbation" displacements  $\delta\Delta$  for which the second variation of vanishes, i. e.,  $\delta\Pi_p = 0$  (Reference 6). Consistent with this, an equilibrium solution for a parametric value of the applied load is obtained from Equation 19. The applied load level for elastic instability is given by the quantity  $\lambda$ , the eigenvalue, times the parametric value of the applied load, and the related internal stresses are those previously designated as  $\bar{\sigma}_1, \bar{\sigma}_2, \bar{\sigma}_{12}$ . The potential energy is then constructed with use of the prebuckling equilibrium stresses and a perturbation displacement field that is consistent with the assumed displacement fields of the respective elements. The result of the application of the condition for neutral stability is

$$\mathbf{K} \delta\Delta + \lambda \mathbf{N} \delta\Delta = \mathbf{0} \quad (21)$$

and, since  $\delta\Delta \neq \mathbf{0}$  for a nontrivial solution

$$|\mathbf{K} + \lambda \mathbf{N}| = \mathbf{0} \quad (22)$$

As noted in conjunction with the discussion of Equation 19, the solution for the prebuckling equilibrium state cannot be accomplished directly. The manner of dealing with this circumstance is most conveniently described in conjunction with a review of the computer program employed in the numerical analysis. This description is given following the definition of a procedure for reducing the order of the eigenvalue determination inferred by Equation 22.

SECTION VI  
REDUCTION PROCEDURE

In view of the expense and questionable accuracy of state of the art eigenvalue calculation subroutines when applied to large-order (>100 degrees of freedom) systems, it is useful to have methods available for the reduction of the order of such systems prior to eigenvalue determination. Exact reduction procedures cannot be defined for the form of equations encountered in the present development; the method sought is therefore approximate in form. A corresponding form of the eigenvalue problem is met in vibrational frequency analysis with the use of consistent mass matrices. Guyon (Reference 23) has presented an approximate method of reducing the order of the latter; the method is now applied to the buckling problem.

The removal of certain degrees of freedom from the problem statement can be regarded as a transformation of coordinates from the complete set of degrees of freedom to the designated reduced number. The procedure described here is based upon the premise that such a transformation of coordinates, derived from consideration of the stiffness matrix in isolation, is suitable as an approximate transformation of the incremental stiffness matrix.

Consider first the analysis of a system excluding elastic instability effects. The formulation is partitioned to distinguish between the degrees of freedom to be removed (subscript e) and those to be retained (subscript f). The former are unloaded degrees of freedom. Thus,

$$\mathbf{K} \Delta = \mathbf{P} \tag{23}$$

or

$$\begin{bmatrix} \mathbf{K}_{ff} & \mathbf{K}_{fe} \\ \mathbf{K}_{ef} & \mathbf{K}_{ee} \end{bmatrix} \begin{bmatrix} \Delta_f \\ \Delta_e \end{bmatrix} = \begin{bmatrix} \mathbf{P}_f \\ \mathbf{0} \end{bmatrix} \tag{24}$$

Solving for  $\Delta_e$  in the lower equation of the partition and insertion of the result in the upper equation yields

$$(\mathbf{K}_{ff} - \mathbf{K}_{fe} \mathbf{K}_{ee}^{-1} \mathbf{K}_{ef}) \Delta_f = \mathbf{P}_f \tag{25}$$

which can also be written in the form of a conventional transformation of coordinates:

$$\mathbf{T}^T \mathbf{K} \mathbf{T} = \mathbf{P}_f \tag{26}$$

where  $\mathbf{T}$  is defined by

$$\begin{bmatrix} \Delta_f \\ \Delta_e \end{bmatrix} = \begin{bmatrix} \mathbf{I} \\ -\mathbf{K}_{ee}^{-1} \mathbf{K}_{ef} \end{bmatrix} \Delta_f = \mathbf{T} \Delta_f \quad (27)$$

In accordance with the view advanced above, the reduced form of the structural stability formulation is

$$(\mathbf{T}^T \mathbf{K} \mathbf{T} - \lambda \mathbf{T}^T \mathbf{N} \mathbf{T}) \Delta_f = \mathbf{0} \quad (28)$$

in which the indicated matrices are partitioned with reference to the degrees of freedom "e" and "f".

The foregoing places no limitation on the selection of the respective groups of degrees of freedom, other than the requirement that the system  $\Delta_f$  correspond to stable support of the structure if it were to be suppressed. In the present applications only the angular  $(\theta_{\alpha_1}, \theta_{\alpha_2})$  and twist  $(\theta_{\alpha_1}, \alpha_2)$  degrees of freedom are removed; the illustrative examples of the next section include numerical evaluation of the approximation embodied in this reduction procedure.



## SECTION VII

## ILLUSTRATIVE EXAMPLES AND ACCURACY COMPARISONS

A concise flow chart of the program for calculation of the results described in this section (Figure 5) serves to clarify the theoretical procedure applied here. It also furnishes a basis for discussion of the key mathematical aspects of the solution process.

Routines for input data, formation of the element and structure matrices, and output were coded directly but maximum utilization was otherwise made of subroutines available in the IBM System/360 Scientific Subroutine Package (Reference 25). (The program was coded in Fortran IV for the Cornell University 360/65 computer system). Direct stiffness concepts (Reference 24) were employed in construction of the matrices for the complete structure.

The Reference 25 matrix inversion subroutine (MINV) represents application of the standard Gauss-Jordan method. The algorithm for computing eigenvalues is that described as NROOT. This subroutine calculates the eigenvectors of a real, square, nonsymmetric matrix of the form  $\mathbf{K}^{-1}\mathbf{N}$ , where both  $\mathbf{K}$  and  $\mathbf{N}$  are real symmetric matrices, by first symmetrizing this product through special transformations and by subsequent application of the Jacobi rotation method (Reference 26).

Examining the program flow, it is seen that the analyst is at liberty either to specify the prebuckling stress distribution or to seek performance of analyses for the purpose of computing these stresses. The former case generally corresponds to a situation wherein the prebuckling stress distribution is computed independently by membrane theory, without reference to geometric boundary conditions. This option was invoked in the calculation of solutions for comparison with the "classical" linear stability solutions.

In performing analyses for prebuckling stresses, the structure stiffness matrix is first calculated and a solution is accomplished for displacements and stresses. The stresses are then employed in construction of the  $\mathbf{N}$  matrix and with this a revised solution is accomplished. The process advances iteratively until the difference between predicted displacements in successive analyses is reduced below a pre-selected tolerance. A tolerance of 0.1% in the values of each term of the displacement vector was used for the analyses performed.

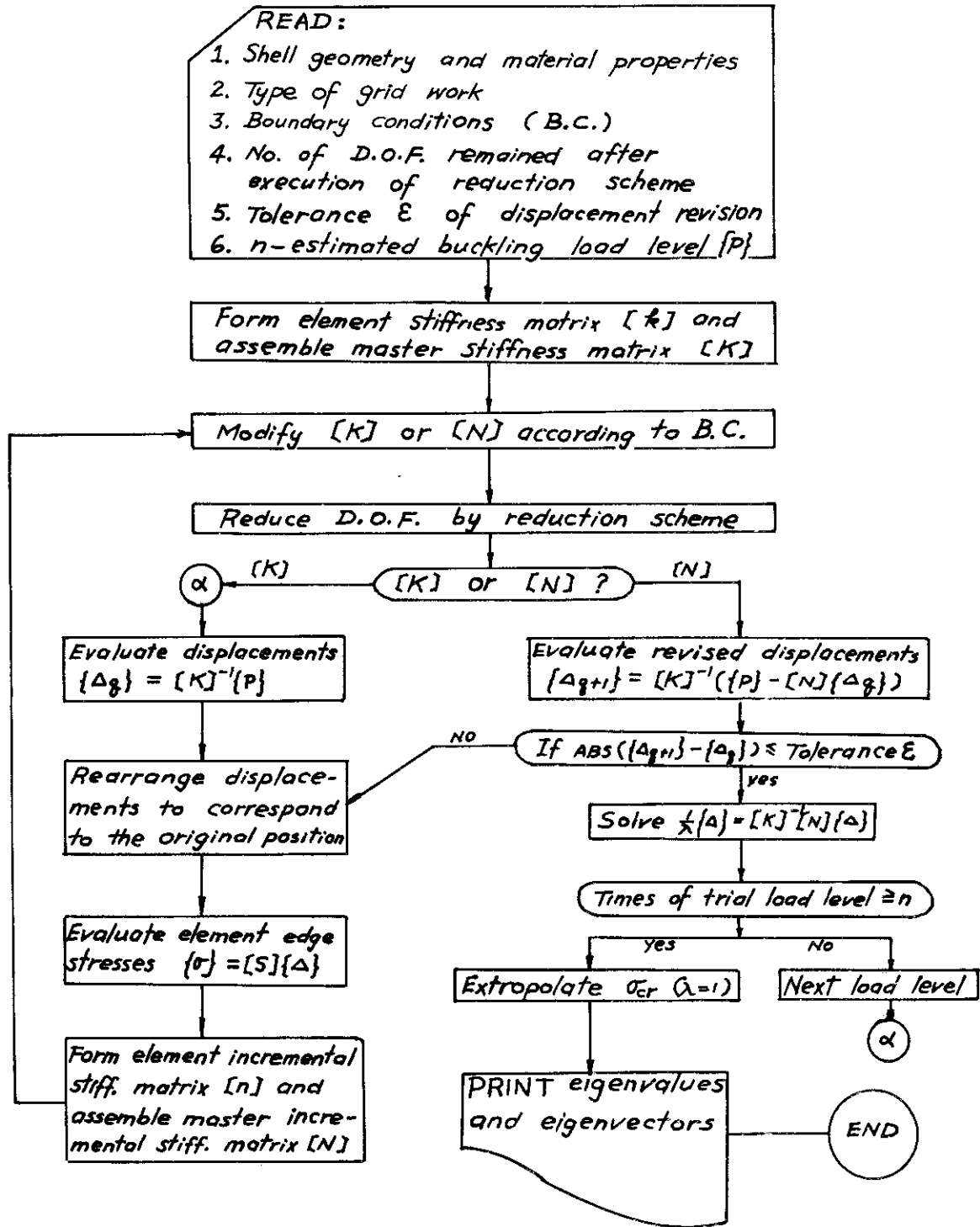


Figure 5. Elastic Instability Analysis Flow Chart

The prebuckling stress should in theory be consistent with the response to the applied load level immediately prior to the bifurcation of equilibrium. A procedure for approximating this closely was advanced in Reference 5 and employed here. Application of this procedure is signified in Figure 5 by the indicated iteration upon the eigenvalue calculation.

The definition of a series of analyses to assess the accuracy of the previously described developments was governed by the following objectives:

- 1) Assessment of the influence upon solution accuracy of the approximate reduction procedure.
- 2) Relative accuracy of the element formulation in applications ranging from the flat plate to doubly curved shell, in comparison with classical solutions.
- 3) Examination of the ability of the element formulation and general analysis procedure to deal with the influence of edge conditions on stability.
- 4) To gain insight into possible special shortcomings of the formulation with reference to specific problems.

Analyses of the simply-supported beam (using element equations derived in Reference 18) and the square rectangular simply-supported plate (based on the subject formulation) were conducted for a series of grid, refinements for both the reduced and unreduced analysis procedures. The  $\theta_{\alpha_1}$ ,  $\theta_{\alpha_2}$  and  $\theta_{\alpha_1 \alpha_2}$  degrees of freedom are removed in reduced analyses, i.e., the problem is stated in terms of the w-displacements alone. Results are shown in Figures 6 and 7. It is seen that the error due to the approximate reduction scheme is negligible for as few as four elements in both cases. The finite element solution itself proves to be quite accurate when compared with the "exact" solution of Reference 27.

Results for the cylindrical shell were obtained entirely with use of the reduction procedure. It should be noted that the condition of continuity of the joint displacement parameters  $\theta_{\alpha_1 \alpha_2}$  was enforced in all cases of plate and shell analysis. The cylindrical shell results appear in Figures 8 and 9 with the idealization gridworks shown in inserts in these figures. All analyses employed symmetry and an idealization within an octant of the complete cylinder.

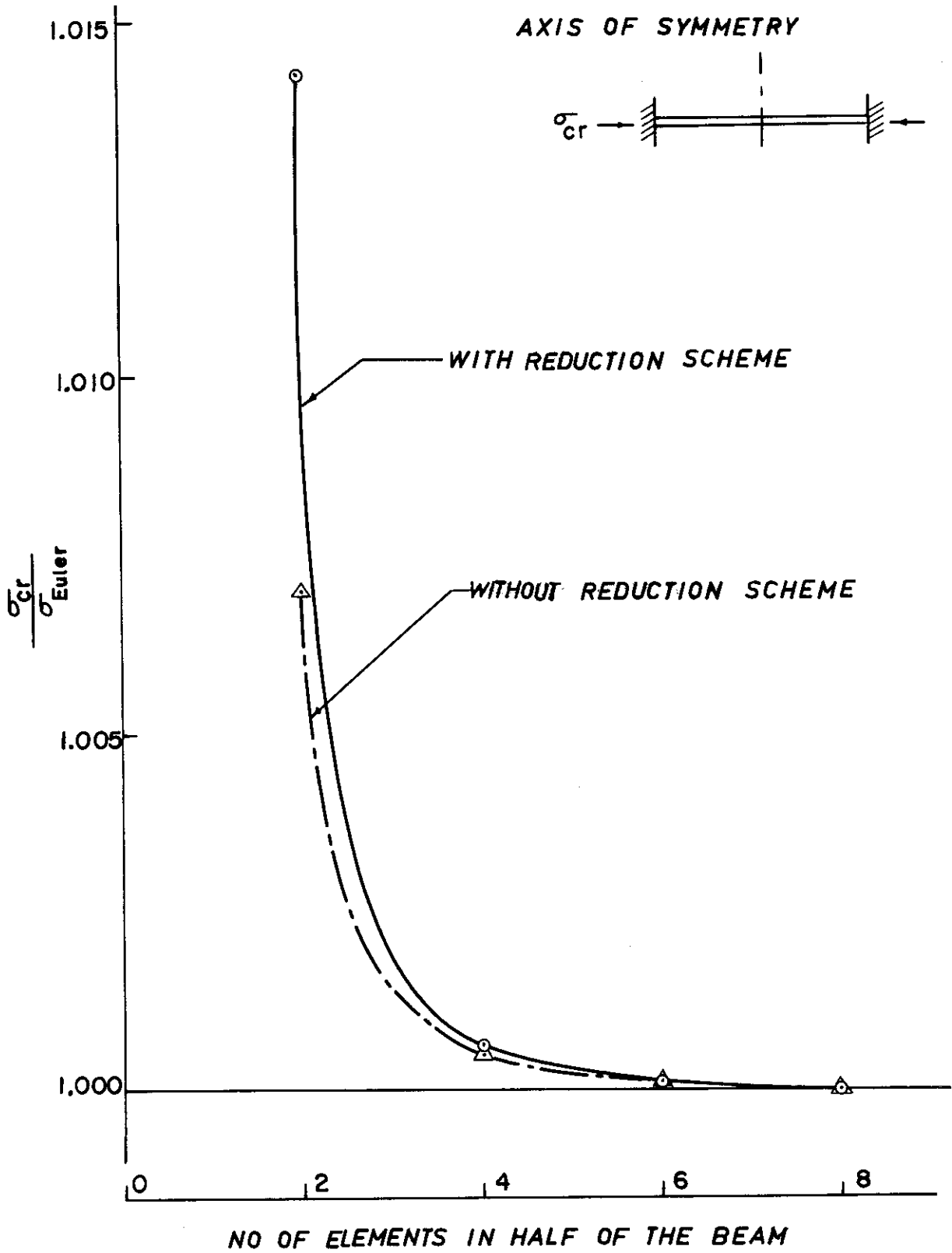


Figure 6. Column Buckling - Accuracy Vs. Grid Refinement

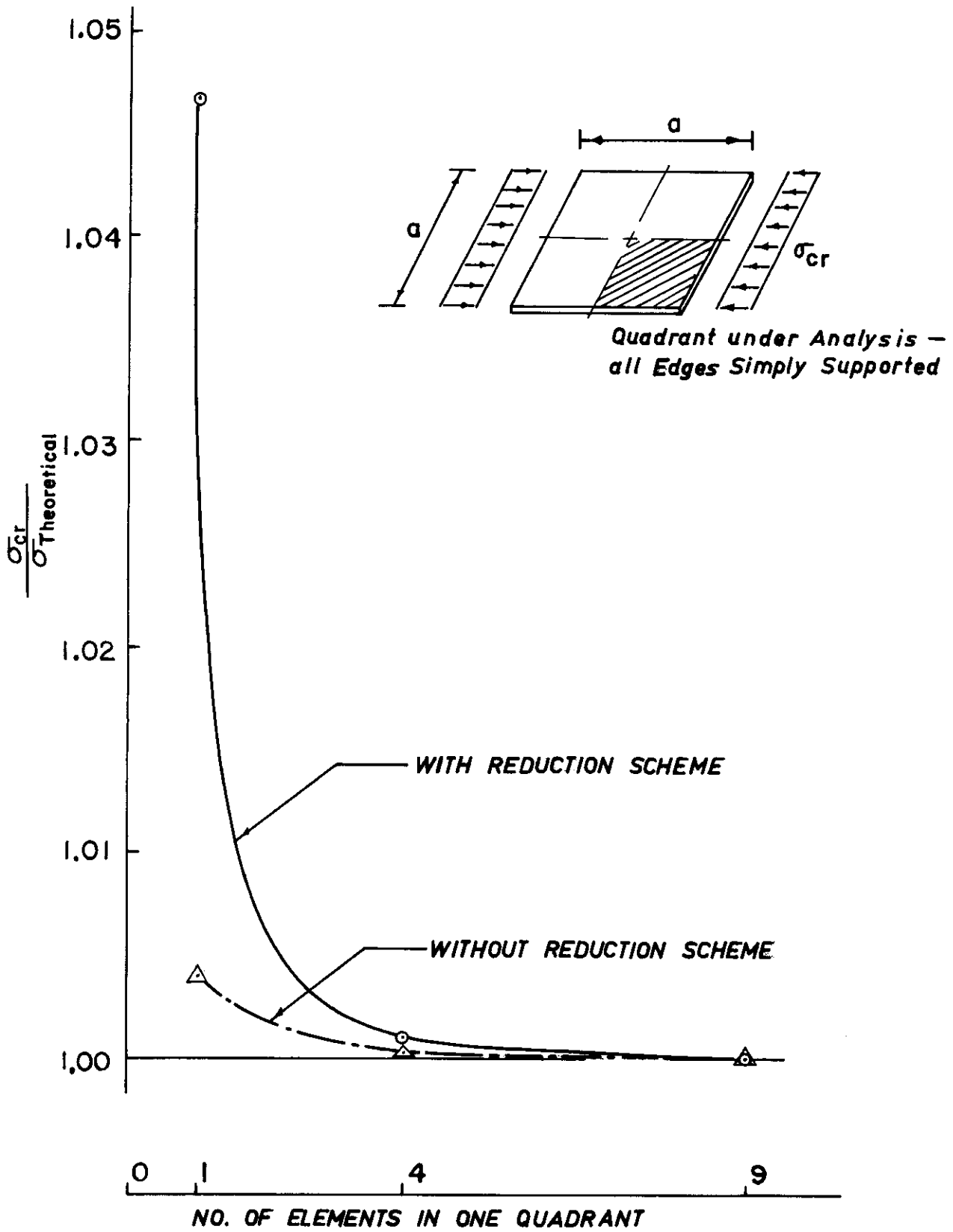


Figure 7. Plate Buckling Accuracy Vs. Grid Refinement

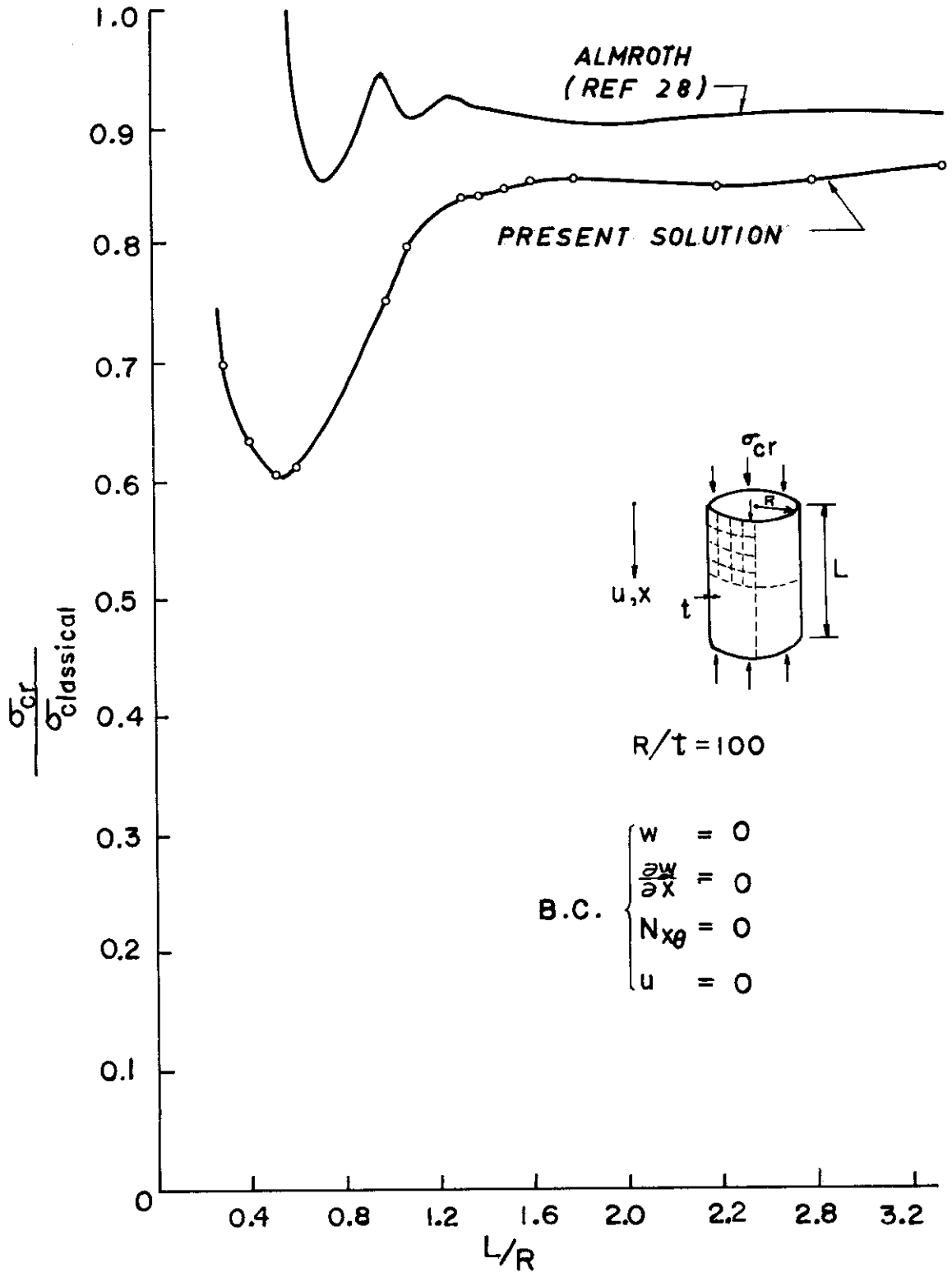


Figure 8. Influence of Shell Length for Clamped Cylinders

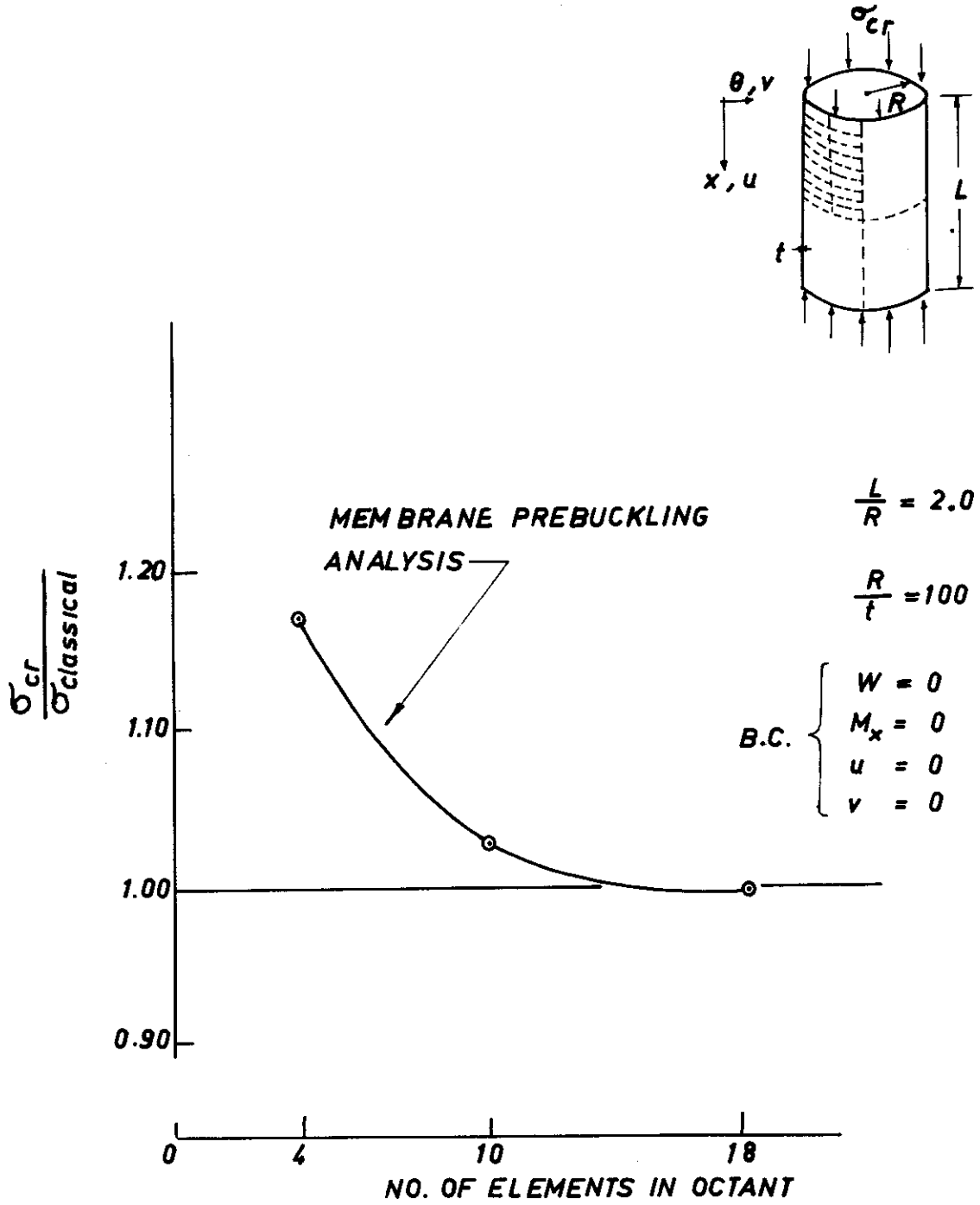


Figure 9. Cylinder Buckling - Accuracy Vs. Grid Refinement

Figure 9 pertains to the effect of grid refinement upon a solution embodying the assumptions of classical linear stability analysis. Thus, the prebuckling deformations are disregarded and membrane theory is applied to define the middle surface stress distribution. The results prove to be in close agreement with the classical solution,  $\sigma_{cr} = 0.605 Et/R$ .

Computations which embody consideration of prebuckling deformations have been performed by Almroth, (Reference 28) using a harmonic representation of circumferential behavior and finite difference approximation for behavior described by the axial coordinate. The problem has also been discussed by Hoff and Soong (Reference 29) and by Stein (Reference 30). A clamped cylinder is chosen for analysis and a fixed number of elements (16) is employed in the idealization. The analyses are performed for 14 different values of the L/R ratio and the results are plotted and compared with those of Almroth in Figure 9. This figure shows that the buckling load becomes independent of the L/R ratio for large values of that parameter and in this region the difference between the present results and those of Reference 28 is approximately 6%. The discrepancies are much larger at the lower values of L/R but the same behavior trends are preserved.

The level of agreement with the results of Reference 28 is felt to be good in the range of high L/R ratios, in view of the crudity of the present finite element gridwork as compared to corresponding considerations in Reference 28. In particular, the prebuckling stress field is highly localized in the support region due to limitations on computer capacity and no attempt is made in the finite element idealization to model this region more accurately. Whether or not the refinement of the gridwork will remove the level of discrepancy is open to question, however. This same type and level of discrepancy is reported by Navaratna, et al, (Reference 6) who used an axisymmetric finite element in calculation of another case examined by Almroth in Reference 28. The computations in these two references can be regarded as being based upon comparable levels of "grid refinement". This particular aspect of cylinder stability analysis merits attention in future finite element shell stability studies.

As a final illustration, the doubly curved shallow shell with rectangular boundaries (Figure 10) is considered. Very few comparison solutions exist for this type of structure. Finite element stability analyses were performed for the concentrated load case (Figure 10b) and are described in Reference 19. These results, due to the absence of a comparison solution, give no measure per se of the accuracy of the element formulation. Other comparison bases have therefore been sought. One has recently appeared in the note by Haydl (Reference 31)



in which the buckling of the doubly curved panel under loads in the x-y plane (Figure 10a) is examined. The problem excludes consideration of prebuckling deformation and derives the following formula for the case shown:

$$(P_x)_{cr} = (P_y)_{cr} = Et / R \left[ 3(1-\mu^2) \right]^{1/2} \quad (29)$$

The plot of the finite element solution (Figure 10) versus the subtended angle shows close agreement of the present formulation with the solution given by Equation 29.

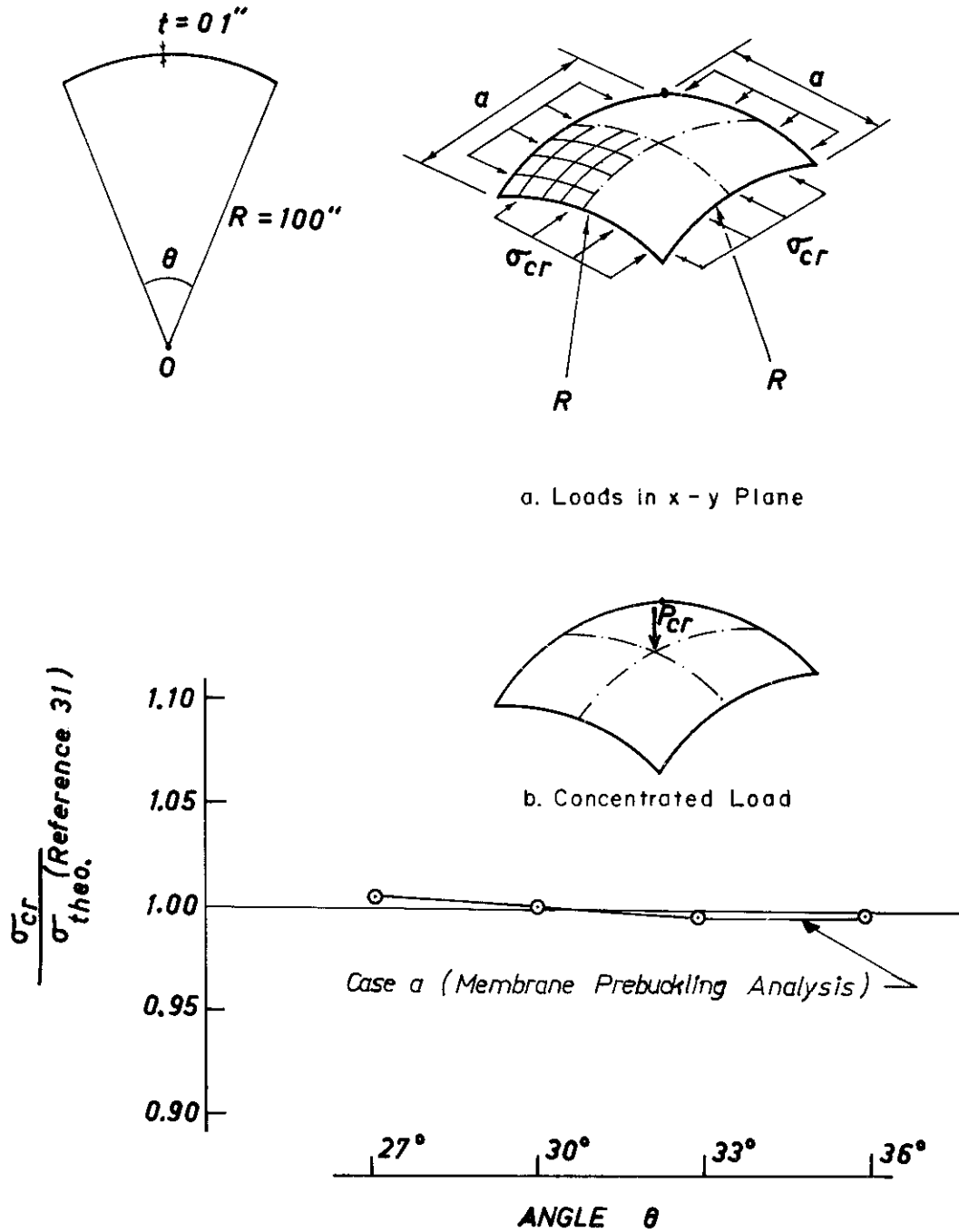


Figure 10. Stability Analysis of Doubly Curved Shells

SECTION VIII  
CONCLUSIONS

The formulation of the stiffness equations described herein for the specified doubly curved shell element has been found to be effective for the prediction of linear stability phenomena of flat plates, cylinders, and more general shapes. Also, the approximate procedure for the reduction of the order of the problem statement has been found to be highly accurate for the circumstances analyzed. The effects of prebuckling deformations on the critical loads of cylinders, a phenomenon of current theoretical interest, has been represented in the finite element solution. The accuracy of the developed formulation in the prediction of this effect could not be defined clearly due to limitations on grid refinement and the approximate nature of the comparison solution itself.

Lack of satisfaction of the pertinent conditions related to rigid body motion in the assumed displacement field, together with inconsistency of the shapes of the membrane and flexure boundary displacements, appeared to have little influence on the solutions obtained. To the extent that it would be desirable to retain the explicit algebraic form of the derived element formulations, the present developments suggest extension to deal with geometric nonlinearities and with the inclusion of terms representative of initial imperfections.

If major improvements are sought in the formulation of a doubly curved shell element for instability analysis, for instance, improved displacement functions, it is apparent that the objective of an explicit algebraic formulation must be abandoned. Numerical integration is dictated, but this immediately opens the possibility of convenient inclusion of improved displacement functions, a more general shape, geometric nonlinearities and other desirable aspects of the problem formulation.

## SECTION IX

## REFERENCES

1. Mallett, R. and Marcal, P., "Finite Element Analysis of Nonlinear Structures", Proc. ASCE, Journal of the Structural Div., No. ST9, Sept. 1968.
2. Oden, J. T., Numerical Formulation of Nonlinear Elasticity Problems", Proc. ASCE, V. 93, No. ST4, Aug. 1967.
3. Martin, H. C., "On the Derivation of Stiffness Matrices for the Analysis of Large Deflection and Stability Problems", Proc. of the AFIT Conference on Matrix Methods in Structural Mechanics, AFFDL TR 66-80, Nov. 1965.
4. Kapur, K and Hartz, B., "Stability of Plates Using the Finite Element Method", Proc. ASCE, Journal of the Engineering Mechanics Division, V. 92, No. EM2, April, 1966.
5. Gallagher, R., Gellatly, R., Mallett, R., and Padlog, J., "A Discrete Element Procedure for Thin Shell Instability Analysis", AIAA Journal, V. 5, No. 1, Jan. 1967.
6. Navaratna, D., Pian, T. and Witmer, E., "Analysis of Elastic Stability of Shells of Revolution by the Finite Element Method", AIAA Journal, V. 6, No. 2, Feb. 1968.
7. Jones, R. and Strome, D., "Direct Stiffness Method of Analysis of Shells of Revolution Utilizing Curved Elements", AIAA Journal, V. 4, No. 9, Sept. 1966.
8. Fulton, R., Eppink, R. and Walz, J., "The Accuracy of Finite Element Methods in Continuum Problems", Proc. Fifth U. S. National Congress of Applied Mechanics, ASME, 1966.
9. Cantin, R. and Clough, R., "A Curved, Cylindrical-Shell Finite Element", AIAA Journal, V. 6, No. 6, June, 1968.
10. Bogner, F., Fox, R. and Schmit, L., "A Cylindrical Shell Discrete Element", AIAA Journal, V. 5, No. 4, April 1967.
11. Bogner, F., Fox, R. and Schmit, L., "Finite Deflection Analysis Using Plate and Cylindrical Shell Discrete Elements", AIAA Journal V. 6, No. 5, May 1968.
12. Gallagher, R., The Development and Evaluation of Matrix Methods for Thin Shell Structural Analysis, Ph.D. Dissertation, State University of New York at Buffalo, June, 1966.
13. Deak, A., Analysis of Shallow Shells by the Displacement Method, Univ. of Washington, College of Engineering, Dept. of Aeronautics and Astronautics, Report 77-4, June, 1967.
14. Connor, J. and Brebbia, C., "Stiffness Matrix for Shallow Rectangular Shell Element", Proc. ASCE, Journal of the Engineering Mechanics Div., No. EM5, Oct. 1967.
15. Utku, S., "Stiffness Matrices for Thin Triangular Elements of Nonzero Gaussian Curvature", AIAA Journal, V. 5, No. 9, Sept. 1967.
16. Szilard, R. and West, A., Finite Curved Shell Elements and Consistent Mass Matrices for Static and Dynamic Analysis of Aerospace Structures, Air Force Flight Dynamics Laboratory Report No. AFFDL TR 66-194.

## REFERENCES (CONTD)

17. Novozhilov, V., The Theory of Thin Shells, P. Noordhoff, Ltd., The Netherlands, 1959.
18. Gallagher, R. and Padlog, J., "Discrete Element Approach to Structural Instability Analysis", AIAA Journal, V. 1, No. 6, June, 1963.
19. Yang, H. T. Y., A Finite Element Formulation for Stability Analysis of Doubly Curved Thin Shell Structures, Ph. D. Dissertation, Cornell University, January, 1969.
20. Zienkiewicz, O. and Cheung, Y., "The Finite Element Method in Structural and Continuum Mechanics", Chapter 2, McGraw-Hill Publishing Co., Ltd., London, 1967.
21. Bogner, F., Fox, R. and Schmit, L., "The Generation of Interelement-compatible Stiffness and Mass Matrices by the Use of Interpolation Formulae", Proceedings of the AFIT Conference on Matrix Methods in Structural Mechanics, AFFDL TR 66-90, Nov. 1965.
22. Haisler, W. and Stricklin, J., "Rigid-Body Displacements of Curved Elements in the Analysis of Shells by the Matrix Displacement Method", AIAA Journal, V. 5, No. 8, Aug. 1967.
23. Gyan, R., "Reduction of Stiffness and Mass Matrices", AIAA Journal, V. 3, No. 2, Feb. 1965.
24. Martin, H., Introduction to Matrix Methods of Structural Analysis, McGraw-Hill Book Co., New York, N. Y., 1966.
25. Anon., "System/360 Scientific Subroutine Package (360A-CM-03X) Version II. Programmers Manual", IBM Applications Program Manual H20-0205-2, 1967.
26. Ralston, A., A First Course in Numerical Analysis, McGraw-Hill Book Co., 1965.
27. Timoshenko, S. and Gere, J., Theory of Elastic Instability McGraw-Hill Book Co., New York, N. Y., 1961.
28. Almroth, B., Influence of Edge Conditions on the Stability of Axially Compressed Cylindrical Shells, NASA CR-161, Feb., 1965.
29. Hoff, N. J. and Soong, T-C., "Buckling of Circular Cylindrical Shells in Axial Compression", Intl. Journal of Mech. Science, V. 7, 1965, pp. 489-520.
30. Stein, M., "Recent Advances in Shell Buckling", AIAA Preprint 68-103, 6th Aerospace Sciences Meeting, New York, N. Y., Jan. 1968.
31. Haydl, H., "Buckling of Doubly-Curved Shallow Thin Shells", AIAA Journal, V. 6, No. 5, May 1968, pp. 982-984.

# *Contrails*